J Therm Anal Calorim (2010) 102:83–90
DOI 10.1007/s10973-010-0748-2

Thermal stability and degradation of Co(II), Cd(II), and Zn(II) complexes with *N*-benzyloxycarbonylglycinato ligand

**Maja T. Šumar-Ristović · Dragica M. Minić ·
Dejan Poleti · Zoran Miodragović ·
Đenana Miodragović · Katarina K. Anđelković**

Received: 15 September 2009 / Accepted: 5 March 2010 / Published online: 24 March 2010

Abstract Thermal behavior of Co(II), Cd(II), and Zn(II) complexes with *N*-benzyloxycarbonylglycinato ligand was investigated using the results of TG, DSC and DTG analysis obtained at different heating rates (2.5 to 30 °C $\min^{-1}$), from room temperature to about 900 °C. Mechanisms of complex degradation, as well as enthalpies of the degradation processes were determined. It is shown that thermal stability of investigated complexes correlates with their crystal structures, especially with the presence of crystallization and coordinated water molecules. The values of dehydration enthalpies are discussed and correlated with composition of the complexes. Kissinger's, Ozawa's, and Friedman's isoconversion methods were used for the determination of kinetic parameters: the pre-exponential factor A and the apparent activation energy E_a. For all three complexes and all steps of degradation, the values of kinetics parameters obtained by Kissinger's and Ozawa's methods are in good agreement. The results obtained by Friedman's method showed that some decomposition steps are simple and some others are complex ones.

Keywords Metal complexes · *N*-benzyloxycarbonylglycine · Thermal analysis · Thermal stability

Introduction

Metal complexes with *N*-substituted amino acids as ligands have attracted a considerable attention of many researches because of their structural and biological properties [1–14]. Interest for biological activity of these complexes is based on the fact that *N*-substituted amino acids represent unique model-systems that contain peptide bond as a part of their structure. Because of that peptide bond, these systems represent good models for investigation of metal ion interactions with peptides, in addition to the study of structural and other properties of some complex systems. It is also very interesting that *N*-benzyloxycarbonyl-protected amino acids and their derivatives were reported as anti-convulsant, anti-inflammatory, and anti-neoplastic agents [4, 10, 15–18]. The investigated *N*-benzyloxycarbonylglycinato ligand, *N*-Boc-gly (Scheme 1), exhibits better anti-convulsant activity than glycine itself [10, 15, 16].

The synthesis, characterization, antimicrobial and antifungal activity of Co(II), Cd(II), and Zn(II) complexes with the *N*-Boc-gly ligand were described previously [19]. The 2D supramolecular structure of Cd(II) complex was resolved by single crystal X-ray analysis. It was found that the cadmium ion has a distorted pentagonal–bipyramidal coordination formed by two water molecules and two *N*-Boc-gly ligands coordinated in different fashions. The first ligand coordinates to only one metal atom as a bidentate chelate, while the second one coordinates three cadmium atoms as a bridging ligand (Scheme 2). On the basis of several techniques (elemental analysis, IR, EA, ^{1}H,

---

M. T. Šumar-Ristović · Z. Miodragović · Đ. Miodragović ·
K. K. Anđelković (✉)
Faculty of Chemistry, University of Belgrade, Studentski trg 16,
11000 Belgrade, Serbia
e-mail: kka@chem.bg.ac.rs

D. M. Minić
Faculty of Physical Chemistry, University of Belgrade,
Studentski trg 16, 11000 Belgrade, Serbia

D. Poleti
Department of General and Inorganic Chemistry, Faculty
of Technology and Metallurgy, University of Belgrade,
Karnegijeva 4, 11000 Belgrade, Serbia

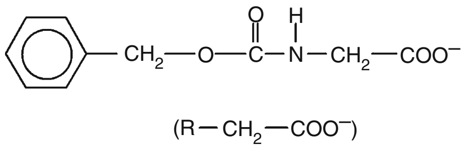

Scheme 1 *N*-benzyloxycarbonylglycinato ligand (*N*-Boc-gly)

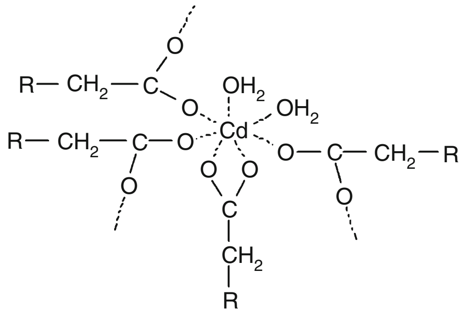

Scheme 2 [Cd(*N*-Boc-gly)$_2$H$_2$O]$_2$

and ^{13}C NMR spectroscopy, magnetic measurements, and DFT), it is concluded that the Zn(II) complex has tetrahedral geometry with two ligands coordinated as O, O chelates, while the Co(II) complex has octahedral geometry with two monodentate ligands in the *trans* position. Investigation of the antimicrobial and antifungal activity revealed that the examined complexes exhibit the best inhibitory activity against *Candida albicans*. Also, Cd(II) complex has an inhibitory activity against *Aspergillus niger*, *Escherichia coli*, and *Micrococcus lysodeicticus*. Although, the great number of literature data for series of coordination compounds of different composition [20–26], there are no data of thermal behavior of these and similar complex systems. Having in mind interesting structural aspects of the complexes with *N*-Boc-gly, as well as their higher antimicrobial activity and selectivity in comparison to the ligand itself, we were inspired for further investigations of thermal behavior of these substances.

Experimental

The investigated Co(II), Cd(II) and Zn(II) complexes with the *N*-Boc-gly ligand and formulae: [Co(*N*-Boc-gly)$_2$(H$_2$O)$_4$]·2H$_2$O, [Cd(*N*-Boc-gly)$_2$(H$_2$O)$_2$], and [Zn(*N*-Boc-gly)$_2$] were prepared in a simple reaction between CoCl$_2$·6H$_2$O, CdCl$_2$·2.5H$_2$O, or ZnCl$_2$ and *N*-Boc-glyH (molar ratio 1:2, ethanol–water mixture at pH 5–6) shown in Scheme 3.

Further details can be found in literature [19].

The experimental data were collected on an SDT Q600 (TA Instruments) apparatus for simultaneous TG-DTA/DSC analysis. The instrument was calibrated by sapphire (for heat capacity), as well as by In and Zn (for temperature and DSC signals). TG/DSC experiments were performed from room temperature to 900 °C with sample masses about 6 mg in a dry nitrogen atmosphere (flow rate: 100 cm^3 min^{-1}). The alumina crucibles, with an empty crucible as a reference, were used. DTG curves at different heating rates (2.5–30 °C min^{-1}) were obtained under similar conditions (mass of the samples: 5–10 mg) in Pt crucibles. A Pt crucible with a small amount of Al$_2$O$_3$ was used as a reference.

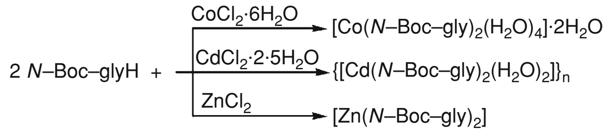

Scheme 3 Reaction scheme of the complexes

Obtained TG, DTG, and DSC results were used to determine the mechanism of decomposition of the complexes, enthalpies of the degradation processes and kinetic parameters (E_a and A).

Results and discussion

Thermal stability and mechanism of degradation

The TG and DTG curves of Co(II), Cd(II), and Zn(II) complexes are shown in Figs. 1, 2, 3, respectively. As seen, degradation of Co and Cd complex occurs in four, whereas degradation of Zn complex occurs in three main steps. In all the cases, some minor steps and asymmetry of DTG/DSC curves were also observed.

It is found that the initial decomposition temperature of the investigated complexes correlates with their structures, especially with the presence of crystallization (lattice) and coordinated water molecules. In this context, the most

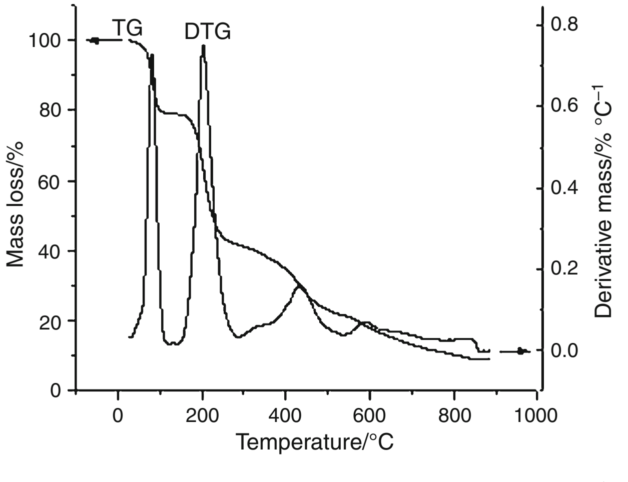

Fig. 1 TG and DTG curves of Co(II) complex (β = 20 °C min^{-1})

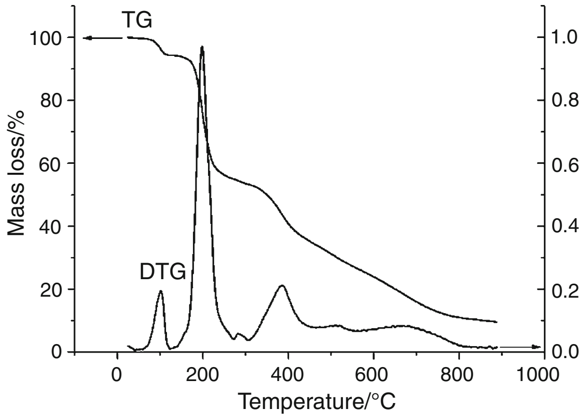

Fig. 2 TG and DTG curves of Cd(II) complex ($\beta = 20$ °C min^{-1})

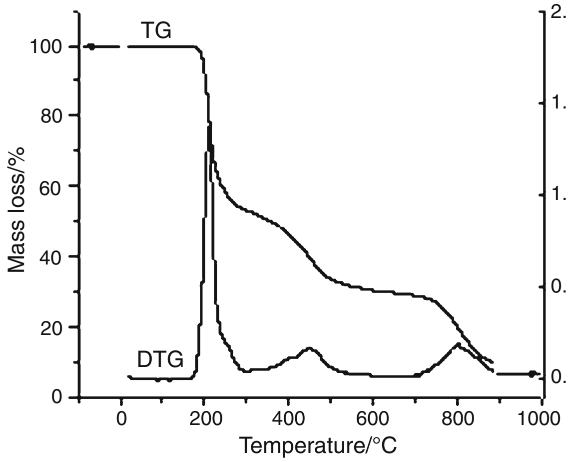

Fig. 3 TG and DTG curves of Zn(II) complex ($\beta = 20$ °C min^{-1})

stable is the Zn(II) complex which has no water molecules in his structure and stays stable up to about 175 °C. The least stable is the Co(II) complex, which has water molecules both in the internal and external sphere, and its degradation starts almost at room temperature. General thermal behavior of the complexes, such as stability ranges, DSC peak temperatures, mass loss data, the corresponding enthalpies at heating range of 20 °C min^{-1} and kinetic parameters (E_a and A) obtained by Kissinger's and Ozawa's methods are listed in Table 1. The calculated activation energies for the first step of decomposition (120.6 for Co(II), 178.3 for Cd(II) and 680.7 kJ mol^{-1} for Zn(II) complex) are in accordance with their thermal stability.

Thermal analysis showed that multi-step decomposition of the Co(II) complex begins practically at room temperature (Fig. 1). A weak peak corresponding to the removal of one water of crystallization (DTG maximum at 36.9 °C) is overlapped with the next peak corresponding to the removal of remaining water molecules (intense sharp DTG peak at 65.3 °C). In next two steps (131–285 and 285–525 °C), decomposition of the ligand chains occurs. The mass loss in the first step can be ascribed to the removal of two $C_6H_5CH_2O$– fragments, while in the second step it can be due to the loss of two –C(=O)NHCH$_2$– fragments of the coordinated ligands. The last stage, in temperature interval 525–900 °C, is connected with loss of two molecules of CO_2.

In the case of Cd(II) complex (Fig. 2), multi-step degradation starts at 63 °C with loss of two molecules of coordinated water. In temperature range 123–269 °C dehydrated complex lose two $C_6H_5CH_2O$– fragments, and ligand chain degradation continues in temperature range 269–461 °C with loss of two –C(=O)NHCH$_2$– fragments. The last stage of degradation (up to 900 °C) is ascribed to loss of two molecules of CO_2 and part of Cd.

Thermal decomposition of the most stable Zn(II) complex (Fig. 3) begins at 175 °C. The first two steps (175–297 and 297–626 °C) are assigned to decomposition of ligand fragments, two $C_6H_5CH_2O$– and two –C(=O)NHCH$_2$– fragments, respectively. Like in the case of Cd(II) complex, the last stage of degradation is corresponding to release of two molecules of CO_2 and part of Zn.

So, we could conclude that defragmentation of ligand chains undergoes by similar mechanism for all three complexes. With regard of these results the suggested mechanisms of thermal degradation, taking in account found and calculated mass loss values (Table 1), we suggested the mechanism of degradation for all three complexes as follows:

$$\begin{aligned}
&\left[\mathrm{M}(N\text{-Boc-gly})_2(\mathrm{H_2O})_n\right]\cdot m\mathrm{H_2O}\\
&\quad\rightarrow \left[\mathrm{M}(N\text{-Boc-gly})_2\right] + (m+n)\mathrm{H_2O}\\
&\quad\rightarrow \left[\mathrm{M}(\mathrm{OOC{-}CH_2{-}NH{-}CO{-}})_2\right] + 2\mathrm{C_6H_5CH_2O}\\
&\quad\rightarrow \left[\mathrm{M}(\mathrm{OOC{-}})_2\right] + 2\text{-C(=O)NHCH}_2 \rightarrow \mathrm{M} + 2\mathrm{CO_2}
\end{aligned}$$

where M = Co, Cd, Zn, $n = 4$, 2, 0, respectively and $m = 2$, 0, 0, respectively. As seen, in addition to the already discussed water removal, the main differences between the investigated complexes are observed in final stages of decomposition. In the case of Co(II) complex the residue is metallic Co; this is a consequence of instability of intermediate products and an inert (N_2) atmosphere in oven. However, the final residuals for Cd(II) and Zn(II) complex are lower than the theoretical values. This indicates that together with removal of CO_2, an evaporation of metals occurs in last step due to low boiling points of Cd and Zn, which are 765 and 907 °C, respectively.

Determination of the apparent activation energy and pre-exponential factor

Kinetics of degradation of the investigated complexes has been studied by applying the Kissinger's and Ozawa's methods in order to determine the pre-exponential factor A and the apparent activation energy E_a.

Table 1 Decomposition temperature ranges, DSC peak temperatures, mass loss data and corresponding enthalpies and kinetic parameters (E_a and A) for Co(II), Cd(II) and Zn(II) complexes with *N*-Boc-gly ligand ($\beta = 20$ °C min^{-1})

Complex	Decomposition temperature range/°C	DSC peak temperature/°C	Mass loss (found)/%	Mass loss (calcd.)/%	Fragment loss	ΔH/kJ mol^{-1}	E_a/kJ mol^{-1} Kissinger; Ozawa	A/min^{-1} Kissinger; Ozawa
Co(II)	30–131	94.9	121.4/20.8	108.0/18.5	$6H_2O$	261.0	120.6; 120.1	2.6×10^{18}; 1.1×10^{16}
	131–285	214.0	218.4/37.5	214.3/36.7	$2C_6H_5CH_2O$–	62.9	134.7; 135.5	8.0×10^{14}; 4.9×10^{12}
	285–525	389.1	114.7/19.7	114.1/19.6	2–C(=O)$NHCH_2$–	110.6	210.2; 210.2	3.0×10^{15}; 1.5×10^{13}
	525–900	≈597, 735[a]	76.4/13.1	72.0/15.1	$2CO_2$	–[a]	–	–
Cd(II)	63–123	110.5	31.6/5.6	36.1/6.4	$2H_2O$	96.4	178.3; 175.4	1.8×10^{25}; 4.0×10^{22}
	123–269	206.5	221.6/39.3	214.3/38.0	$2C_6H_5CH_2O$–	60.8	118.9; 120.3	2.0×10^{13}; 1.5×10^{11}
	269–461	379.0	117.5/20.8	114.1/20.2	2–C(=O)$NHCH_2$–	46.0	260.7; 258.1	7.9×10^{20}; 2.5×10^{18}
	461–900	≈523, 754[a]	134.3/23.8	–	$2CO_2$ + part of Cd[b]	–[a]	–	–
Zn(II)	175–297	213.8	224.5/46.6	214.3/44.5	$2C_6H_5CH_2O$–	155.0	680.7; 654.8 ($\beta = 2.5$–15 °C/min)	1.6×10^{74}; 4.2×10^{70} ($\beta = 2.5$–15 °C/min)
							434.7; 421.0 ($\beta = 20$–30 °C/min)[c]	4.5×10^{47}; 2.9×10^{44} ($\beta = 20$–30 °C/min)[c]
	297–626	464.0	111.7/23.2	114.1/23.7	2–C(=O)$NHCH_2$–	65.8	277.6; 275.2	1.4×10^{20}; 4.8×10^{17}
	626–900	752.0	97.3/20.2	–	$2CO_2$ + part of Zn[b]	474.1	168.0; 176.2	5.0×10^{7}; 9.5×10^{5}

[a] These values could not be precisely determined because weak endothermic DSC peaks at high temperature are not well resolved

[b] About 50% of Cd and 27% of Zn were also evaporated in this step

[c] See text for explanation

The method proposed by Kissinger [27] is based on the functional dependence of the heating rate (β) and variation of the DTG peak maximum temperature in thermograms, supposing that $T_{\max}$ is in proportion to the maximum rate of the reaction and equation:

$$\log\frac{\beta}{T_{\max}^2} = \log\frac{AR}{E_\mathrm{a}} - \frac{E_\mathrm{a}}{2,303 \cdot RT_{\max}}. \quad (1)$$

Plotting the left side of this equation against $1/T_{\max}$ should give a straight line of the slope $-E_\mathrm{a}/2.303R$ and intercept $\log AR/E_\mathrm{a}$. In order to apply this method, it is necessary to perform several thermal analyses of the same substance at different heating rates.

The Ozawa's method [28] is based on the same assumptions and the following equation:

$$\log\beta = \log\frac{AE_\mathrm{a}}{R} - 2.315 - 0.4567\left(\frac{E_\mathrm{a}}{RT_{\max}}\right). \quad (2)$$

The plot $\log\beta$ versus $1/T_{\max}$ should be a straight line and its slope can be used to evaluate the apparent activation energy and intercept to evaluate pre-exponential factor. Once again, it is neccessary to perform several thermal analyses of the same substance at different heating rates, in order to apply this method. The results of evaluations of apparent activation energies and pre-exponential factors by using these two methods are in perfect conformity and are listed in Table 1.

Moreover, taking into account the dependence of activation energy on extent of reaction, as well as the complexity of the solid-state decomposition reactions, for determination of kinetics parameters we used Friedman's isoconversion method known as "model free method" [29]. The basic assumption of the method is that the reaction rate at a constant conversion value, α, is only a function of temperature. This premise supposes possibility of determination of kinetic parameters, $E_{\mathrm{a},\,\alpha}$, and A_α, for each value of α over the entire reaction range. The method does not require any assumption on the function depending on the particular reaction mechanism, and it is based on equation:

$$\ln\left[\beta_i\left(\frac{\mathrm{d}\alpha}{\mathrm{d}T}\right)_{\alpha,i}\right] = \ln[A_\alpha f(\alpha)] - \frac{E_\mathrm{a}}{RT_{\alpha,i}} \quad (3)$$

where the subscript α designates values related to a given extent of reaction, and i is the number of non-isothermal experiment conducted at the heating rate β_i. By plotting $\ln[\beta_i(\mathrm{d}\alpha/\mathrm{d}T)_{\alpha,i}]$ against $1/T_{\alpha,\ i}$, the value of $-E_\mathrm{a}/R$ for a given value of α can be directly obtained. The extent of reaction could be expressed as $\alpha = S_T/S$, where S is the total area between the temperature T_i where the degradation is just started and the temperature T_f where the degradation is completed, and S_T is the area between the initial temperature and a generic temperature, T, ranging between T_i and T_f.

Almost constant values of activation energies for the first step in the case of Cd(II) complex and for the second step in the case of Co(II), Cd(II) and Zn(II) complexes, in the wide range of α values, indicate that these steps are not a complex ones (Fig. 4). However, the obtained values for activation energies show a complex nature of the first step of degradation of Co(II) and Zn(II) complexes and third step of degradation for Co(II), Cd(II) and Zn(II) complexes (Table 2). These steps involve several sub-steps occurring with similar values of activation energy.

Discussion of results

In the case of Co(II) complex the loss of six water molecules significantly changes its structure and octahedral geometry, probably to the tetrahedral one, with coordination number decreasing from six to four. At the same time, the increase of temperature causing the loss of two water molecules disturbs polymeric structure of Cd(II) complex with changing coordination number from seven to five. Degradation mechanisms of these two complexes are similar: I step is loss of water molecules, II and III steps are loss of the same fragments from ligand chains. In the case of the most stable tetrahedral Zn(II) complex, involving only two bidentately coordinated ligands, fragmentation of ligand chains begins at about 175 °C. This explains a lower thermal stability of dehydrated Co(II) and Cd(II) complexes, where fragmentation of ligands starts at 131 and 123 °C, respectively, in comparison to Zn(II) complex with degradation starting at 175 °C. Similar behavior was observed within a series of transition metal complexes with polycarboxylate ligands, where complexes obtained as

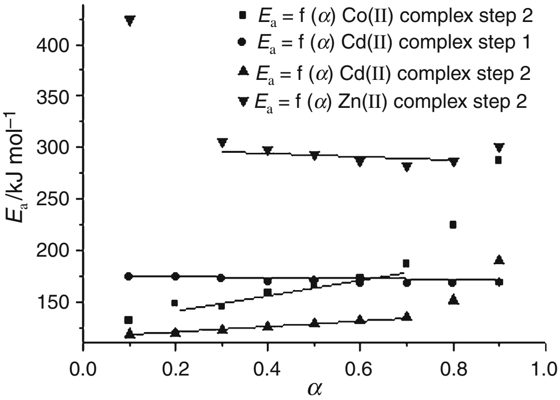

Fig. 4 Functional dependence of the activation energy, E_a, against extent of conversion, α, for first step of degradation of Cd(II) complex and for second step of degradation of Co(II), Cd(II), and Zn(II) complexes

Table 2 Dependence of the activation energy (E_a) against extent of conversion (α) for Co(II), Cd(II) and Zn(II) complexes

α	E_a/kJ mol^{-1}								
	Co(II) complex			Cd(II) complex			Zn(II) complex		
	Step 1	Step 2	Step 3	Step 1	Step 2	Step 3	Step 1	Step 2	Step 3
0.1	114.7	131.6	213.3	174.5	118.8	206.9	–	424.3	181.9
0.2	108.6	148.0	198.4	174.7	119.7	214.7	–	346.3	175.7
0.3	101.5	144.9	252.2	173.1	122.6	230.6	–	305.1	155.5
0.4	91.2	159.0	219.9	170.1	125.9	242.2	558.0	297.5	127.7
0.5	80.5	165.2	218.8	170.3	128.6	247.3	430.5	292.8	102.5
0.6	72.9	172.3	222.3	168.4	132.3	247.9	340.4	286.7	85.2
0.7	70.3	186.8	232.8	167.9	135.9	244.0	258.9	282.8	72.1
0.8	77.4	224.5	230.6	168.2	151.6	232.8	182.2	287.1	69.3
0.9	87.0	286.8	259.7	168.5	189.7	213.6	149.9	301.3	105.3

anhydrous compounds or polymeric complexes were more stable than similar crystalohydrates [30].

The molar dehydratation enthalpy for Co(II) complex (261.0 kJ mol^{-1}) is considerably higher than for Cd(II) complex (96.4 kJ mol^{-1}), what was expectable because the first complex contains six water molecules (two crystal and four coordinated) and the second one contains only two molecules of coordinated water. Having in mind the number of water molecules in the structures of Co(II) and Cd(II) complexes we could calculate the average molar enthalpies of dehydration per one water molecule as 43.5 and 48.2 kJ mol^{-1}, respectively. A slightly higher value for Cd(II) complex in comparison to Co(II) complex is because the Cd(II) complex contains only coordinated water molecules, which should be more tightly bonded than water of crystallization.

If we assume that the elimination of coordinated water molecules from Co(II) and Cd(II) complexes needs the same energy, then using the above calculated value of 48.2 kJ mol^{-1}, the overall enthalpy for removing four coordinated water molecules from Co(II) complex requires $4 \times 48.4 = 192.8$ kJ mol^{-1}. This gives 261.0–192.8 = 68.3 kJ mol^{-1} for two molecules, and 68.2/2 = 34.1 kJ mol^{-1} as the molar enthalpy of dehydration per one crystallization water molecule in Co(II) complex. Since each water molecule very likely takes place in two hydrogen bonds the average molar enthalpy of *per* one hydrogen bond would be about 17 kJ mol^{-1}. This result is in excellent agreement with previous values obtained for energy of hydrogen bond, $\approx$16 kJ mol^{-1}, in some ternary transition metal complexes with terephthalate ligands [31].

For the first step of degradation of ligand chains, the values of molar enthalpies for Co(II) and Cd(II) complexes are almost the same (62.9 and 60.8 kJ mol^{-1}, respectively), indicating a similar mechanism of degradation of ligands in already disturbed structure of complexes. The high value of molar enthalpy for the first step of degradation of ligand chain for Zn(II) complex (155.0 kJ mol^{-1}) is a consequence of very stable structure of this complex involving coordination of metal ion by oxygen atoms from *N*-Boc-gly ligand only.

In the case of Zn(II) complex, the shape of DTG curve for the first step of degradation varies with different heating rates (Fig. 5). Therefore, the kinetic parameters were determined separately for lower (2.5, 5.0, 10, and 15 °C) and higher (20, 25, and 30 °C) heating rates. Again the values obtained by two applied methods are in good agreement (Table 1). Variation of peak shapes and different kinetic parameters for higher and lower heating rates indicate the influence of heating rate on kinetics of the process.

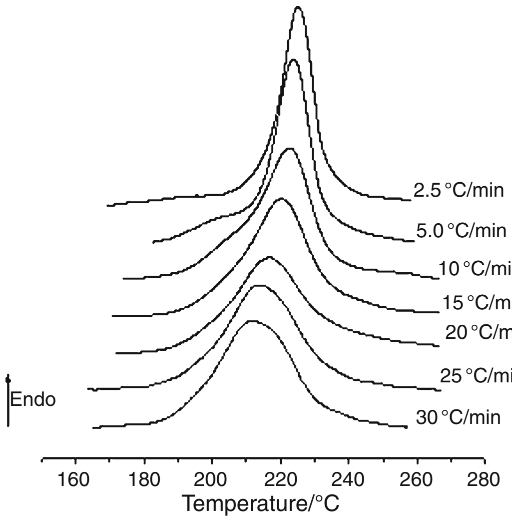

Fig. 5 DTG curves for the first peak of degradation of Zn(II) complex for different heating rates

Conclusions

Co(II), Cd(II) and Zn(II) complexes with the *N*-benzyloxycarbonylglycinato ligand of formulae: $[Co(N\text{-Boc-gly})_2(H_2O)_4]\cdot 2H_2O$, $[Cd(N\text{-Boc-gly})_2(H_2O)_2]$, and $[Zn(N\text{-Boc-gly})_2]$ were thermally investigated. The decomposition of the Co(II) and Cd(II) complexes occurs in four and decomposition of Zn(II) complex occurs in three main steps. The suggested mechanisms of thermal degradation showed that Co(II), Cd(II), and Zn(II) complexes have the same fragmentation of its ligand chains. TG curves revealed that the presence of crystallization and/or coordinated water molecules decreases thermal stability of the complexes. The observed order of decreasing stability is: $[Zn(N\text{-Boc-gly})_2] > [Cd(N\text{-Boc-gly})_2(H_2O)_2] > [Co(N\text{-Boc-gly})_2(H_2O)_4]\cdot 2H_2O$, and the same trend is found after dehydration of Co(II) and Cd(II) complexes. With regard to the composition and structures of complexes, it is confirmed that the loss of crystallization and/or coordinated water molecules cause a disturbance of crystal and molecular structure of the complexes resulting in thermal instability of dehydrated complexes. For the determination of the apparent activation energy (E_a) and pre-exponential factor (A) Kissinger's and Ozawa's methods are used and results of these two methods are in well accordance. Friedman's method signify that the first step of degradation in the case of Cd(II) complex and the second step in the case of Co(II), Cd(II), and Zn(II) complexes are not complex in nature, whereas the first step of degradation of Co(II) and Zn(II) complexes and third step of Co(II), Cd(II), and Zn(II) complexes are the complex ones. A detailed characterization of individual steps will be the subject of further systematic investigations.

Acknowledgements This work was supported by the Ministry of Science and Technological Development of the Republic of Serbia, Grant Nos. 142062 and 142030.

References

1. Sharrok P, Thibaundeau CH, Caille A. Magnetic studies of two new copper hippurate dimers. Inorg Chem. 1971;18:510–2.
2. Battistuzzi Gavioli G, Benedeti L, Grandi G, Marcotrigiano G, Pellacani GC, Tonelli M. Comparison of the polographic behavior of the Cd^{2+}-glycine, *N*-acetyl- and *N*-benzoyl-glycine systems in aqueous and ethanolic solution. Inorg Chim Acta. 1979; 37:5–9.
3. Sajadi Z, Almahood M, Loeffler LJ, Hall IH. Antitumor and antiinflammatory agents: *N*-benzoyl-protected cyanomethyl esters of amino acids. J Med Chem. 1971;22:1419–22.
4. Antolini L, Menabue L, Saladini M, Sola M, Bataglia LP, Corradi AB. Imidazole-containing ternary complexes of *N*-benzyloxycarbonyl-aminoacids. Crystal and molecular structure of bis(*N*-benzyloxycarbonyl-alaninato)bis-(*N*-methylimidazole)copper(II) ethanol solvate. Inorg Chim Acta. 1984;93:61–6.
5. Bataglia LP, Corradi AB, Marcotrigiano G, Menabue L, Pellacani GC. Copper(II) complexes of nitrogen-protected amino acids: synthesis and spectroscopic, magnetic, and structural properties of bis(*N*-acetyl-β-alaninato)diaquacopper(II) and tetrakis[μ-(*N*-acetyl-β-alaninato)]-diaquadicopper(II) dihydrate. A case of structural isomerism. Inorg Chem. 1981;20:1075–80.
6. Antolini L, Menabue L, Prampolini P, Saladini M. Magnetic and spectroscopic properties of dimeric copper(II)*N*-benzoylvalinates. J Chem Soc Dalton Trans. 1982; 2109-12.
7. Cariati F, Erre L, Micera G, Menabue L, Prampolini P. Magnetic investigations on some copper(II) *N*-acetyl- and *N*-benzoyl-alaninates. Inorg Chim Acta. 1982;63:85–9.
8. Udupa MR, Krebs B. Crystal and molecular structure of tetra-μ-*N*-acetylglycinatodiaquodicopper(II). Inorg Chim Acta. 1979; 37:1–4.
9. Anagnostopulos A, Hadjispyrou S. Effects of mixed-ligand complex formation on deprotonation of amide groups in *N*-benzoylglycine and *N*-(4-aminobenzoyl)glycine. J Inorg Biochem. 1995;57:279–86.
10. Lambert DM, Geurts M, Scriba GKE, Poupaert JH, Dumont P. Simple derivatives of amino acid neurotransmitters. Anticonvulsant evaluation of derived amides, carbamates and esters of glycine and β-alanine. J Pharm Belg. 1995;50:194–203.
11. Chikaraishi Kasuga NC, Yamamoto R, Hara A, Amano A, Nomiya K. Molecular design, crystal structure, antimicrobial activity and reactivity of light-stable and water-soluble Ag–O bonding silver(I) complexes, dinuclear silver(I) *N*-acetylglycinate. Inorg Chim Acta. 2006;359:4412–6.
12. Nomiya K, Takahashi S, Noguchi R, Nemoto S, Takayama T, Oda M. Synthesis and characterization of water-soluble silver(I) complexes with L-histidine (H_2his) and (S)-(−)-2-pyrrolidone-5-carboxylic acid (H_2pyrrld) showing a wide spectrum of effective antibacterial and antifungal activities. Crystal structures of chiral helical polymers $[Ag(Hhis)]n$ and $\{[Ag(Hpyrrld)]_2\}n$ in the solid state. Inorg Chem. 2000;39:3301–11.
13. Nomiya K, Takahashi S, Noguchi R. Water-soluble silver(I) complexes of (*R*)-(+)- and (*S*)-(–)-2-pyrrolidone-5-carboxylic acid and their antimicrobial activities. Chiral helical polymer and polymer sheet structures in the solid-state formed by self-assembly of dimeric $[Ag(Hpyrrld)]_2$ cores. J Chem Soc Dalton Trans. 2000;4369-73.
14. Nomiya K, Takahashi S, Noguchi R. Synthesis and crystal structure of three silver(I) complexes with (*S*)-(+)-5-oxo-2-tetrahydrofurancarboxylic acid (S-Hothf) and its isomeric forms (R-Hothf and R,S-Hothf) showing wide spectra of effective antibacterial and antifungal activities. Chiral helical polymers in the solid state formed by self-assembly of the dimeric $[Ag(othf)]_2$ cores. J Chem Soc Dalton Trans. 2000;1343-8.
15. Geurts M, Poupaert JH, Scriba GKE, Lambert DM. *N*-(benzyloxycarbonyl)glycine esters and amides as new anticonvulsants. J Med Chem. 1998;41:24–30.
16. Sussan S, Dagan A, Bialer M. Pharmacokinetic analysis and anticonvulsant activity of glycine and glycinamide derivatives. Epilepsy Res. 1998;33:11–21.
17. Lambert DM, Scriba GKE, Poupaert JH, Dumont P. Anticonvulsant activity of ester- and amide-type lipid conjugates of glycine and *N*-benzyloxycarbonylglycine. Eur J Pharm Sci. 1996; 4:159–66.
18. Koch W, Scheer M, Wolke U, Kaiser A. United States Patent Appl. No. 189:371, 1971.
19. Miodragović ĐU, Mitić DM, Miodragović ZM, Bogdanović GA, Vitnik ŽJ, Vitorović MD, et al. Syntheses, characterization and antimicrobial activity of the first complexes of Zn(II), Cd(II) and Co(II) with *N*-benzyloxycarbonylglycine: X-ray crystal structure of the polymeric Cd(II) complex. Inorg Chim Acta. 2008;361:86–94.
20. Bakalova A. Thermal and spectroscopic investigation of new binuclear Pt(II) complexes with carboxylic acids. J Thermal Anal Calorim. 2009;96:593–7.

21. Patron L, Carp O, Mindru I, Marinescu G, Segal E. Iron, nickel and zinc malates coordination compounds synthesis, characterization and thermal behaviour. J Thermal Anal Calorim. 2003;72:281–8.
22. Jisha KR, Suma S, Sudarsanakumar MR. Synthesis, spectral characterisation and thermal studies of zirconyl complexes of biologically active molecules. J Thermal Anal Calorim. 2010;99:509–13.
23. Luan SR, Zhu YH, Jia YQ, Cao Q. Characterization and thermal analysis of thiourea and bismuth trichloride complex. J Thermal Anal Calorim. 2010;99:523–30.
24. Soliman MH, Mohamed GG, Mohamed EA. Metal complexes of fenoterol drug. J Thermal Anal Calorim. 2010;99:639–47.
25. Tian L, Ren N, Zhang JJ, Liu HM, Sun SJ, Ye HM, et al. Synthesis and thermal decomposition kinetics of two lanthanide complexes with cinnamic acid and 2,2′-bipyridine. J Thermal Anal Calorim. 2010;99:349–56.
26. Bakalova A, Varbanov H, Buyukliev R, Momekov G, Ivanov D. Palladium(II) complexes with 5-methyl-5-(4-pyridyl)-2,4-imidazolidenedione synthesis, thermogravimetric and cytotoxic investigation. J Thermal Anal Calorim. 2009;95:241–6.
27. Kissinger HE. Reaction kinetics in differential thermal analysis. Anal Chem. 1957;29:1702–6.
28. Ozawa T. Kinetic analysis of derivative curves in thermal analysis. J Thermal Anal Calorim. 1970;2:301–24.
29. Friedman HL. Kinetics of thermal degradation of char-forming plastics from thermogravimetry—application to a phenolic resin. J Polym Sci C. 1964;6:183–95.
30. Poleti D, Stojaković Đ. The thermal behavior of ternary cobalt(II), nickel(II) and copper(II) complexes with phthalate ion and 1,10-phenanthroline or 2,2′-dipyridylamine. Thermochim Acta. 1992;205:225–33.
31. Rogan J, Poleti D. Thermal behaviour of mixed ligand Co(II), Ni(II) and Cu(II) complexes containing terephthalate ligands. Thermochim Acta. 2004;413:227–34.